LETTER

doi:10.1038/nature10930

Coherent quantum phase slip

O. V. Astafiev[1,2], L. B. Ioffe[3], S. Kafanov[1,2], Yu. A. Pashkin[1,2,4], K. Yu. Arutyunov[5,6], D. Shahar[7], O. Cohen[7] & J. S. Tsai[1,2]

A hundred years after the discovery of superconductivity, one fundamental prediction of the theory, coherent quantum phase slip (CQPS), has not been observed. CQPS is a phenomenon exactly dual[1] to the Josephson effect; whereas the latter is a coherent transfer of charges between superconducting leads[2,3], the former is a coherent transfer of vortices or fluxes across a superconducting wire. In contrast to previously reported observations[4–8] of incoherent phase slip, CQPS has been only a subject of theoretical study[9–12]. Its experimental demonstration is made difficult by quasiparticle dissipation due to gapless excitations in nanowires or in vortex cores. This difficulty might be overcome by using certain strongly disordered superconductors near the superconductor–insulator transition. Here we report direct observation of CQPS in a narrow segment of a superconducting loop made of strongly disordered indium oxide; the effect is made manifest through the superposition of quantum states with different numbers of flux quanta[13]. As with the Josephson effect, our observation should lead to new applications in superconducting electronics and quantum metrology[1,10,11].

Phase slips across superconducting wires[14] lead to non-zero resistance[2,15]; they may also lead to qubit dephasing, as result of charge noise[16] in a chain of Josephson junctions[17]. Resistance measurements are dissipative, so its saturation at low temperatures cannot be interpreted as evidence for coherent QPS; however, a blockade of supercurrent might indicate CQPS, as demonstrated in ref. 8. A system decoupled from the environment has been suggested[13]: a superconducting loop in which phase slips change the number of quantized fluxes[18], resulting in their quantum superposition, therefore, exhibiting CQPS[9]. We report a successful implementation of this idea using superconducting loops made of highly disordered InO_x.

We begin by considering a superconducting loop of effective area S with a high kinetic inductance L_k, containing a narrow segment (nanowire) with a finite rate of QPS. The external magnetic field B_{ext} perpendicular to the loop induces a flux $\Phi_{ext} = B_{ext}S$. The states of the loop are described by the phase winding number, N; their energies are $E_N = (\Phi_{ext} - N\Phi_0)^2/2L_k$ (Fig. 1a). The energy difference between adjacent states $|N+1\rangle$ and $|N\rangle$ is $E_{N+1} - E_N = 2I_p\delta\Phi$, where $\delta\Phi = \Phi_{ext} - (N+1/2)\Phi_0$ and $I_p = \Phi_0/2L_k$ is the loop persistent current. At $\delta\Phi = 0$, the two states are degenerate. The QPS process, characterized by the amplitude E_S, couples the flux states, resulting in the Hamiltonian

$$H = -\frac{1}{2}E_S(|N+1\rangle\langle N| + |N\rangle\langle N+1|) + E_N|N\rangle\langle N| \qquad (1)$$

which is dual to the Hamiltonian of a superconducting island connected to a reservoir through a Josephson junction. In the latter, L_k is replaced by capacitance, E_S by the Josephson energy, and N is the number of the Cooper pairs on the island[13]. The energy splitting between the ground and excited states $|g\rangle = \sin\frac{\theta}{2}|N\rangle + \cos\frac{\theta}{2}|N+1\rangle$ and $|e\rangle = \cos\frac{\theta}{2}|N\rangle - \sin\frac{\theta}{2}|N+1\rangle$ is $\Delta E = \sqrt{(2I_p\delta\Phi)^2 + E_S^2}$, where the mixing angle is $\theta = \arctan[E_s/(2I_p\delta\Phi)]$.

To detect CQPS, the loop is coupled to the coplanar line (resonator) by mutual inductance, M (ref. 19). In a rotating wave approximation, the effective Hamiltonian of the system resonantly driven by a classical microwave field with current amplitude $I_{mw}\cos(\Delta Et/\hbar)$ is $H_{rw} = \frac{\hbar\Omega}{2}(|e\rangle\langle g| + |g\rangle\langle e|)$, where $\hbar\Omega = MI_pI_{mw}\frac{E_S}{\Delta E}$ and $\hbar$ is the reduced Planck's constant, $h/2\pi$. Note that a transition between the two states can be induced only when $E_S \neq 0$, so observation of the spectroscopy peak constitutes direct evidence for CQPS.

Now we provide theoretical background for our choice of material. CQPS results from quantum fluctuations of the order parameter. Generally, the impact of fluctuations is characterized by the Ginzburg parameter, G_i, which is essentially the inverse number of Cooper pairs in a volume ξ^3: $G_i = (\xi^3\nu\Delta)^{-1}$, where ν is the electron density of states, Δ is the superconducting gap and ξ is the coherence length. Even in disordered bulk superconductors characterized by $k_Fl \approx 1$ (where k_F is the Fermi wavevector and l is the mean free path), G_i is small: $G_i \approx (k_F\xi)^{-1} \ll 1$. Strong fluctuations require materials with an even higher degree of disorder, in which electrons are localized. The superconductivity is suppressed if the localization length, ξ_{loc}, becomes shorter than ξ. Following this reasoning, we expect that the fluctuations are maximal ($G_i \approx 1$), when $\xi_{loc} \approx \xi$, that is, close to the superconductor–insulator transition. Although BCS theory[2] fails to describe this transition, it provides a qualitatively correct explanation for the behaviour of materials with $\xi_{loc} \approx \xi$. The fluctuations are

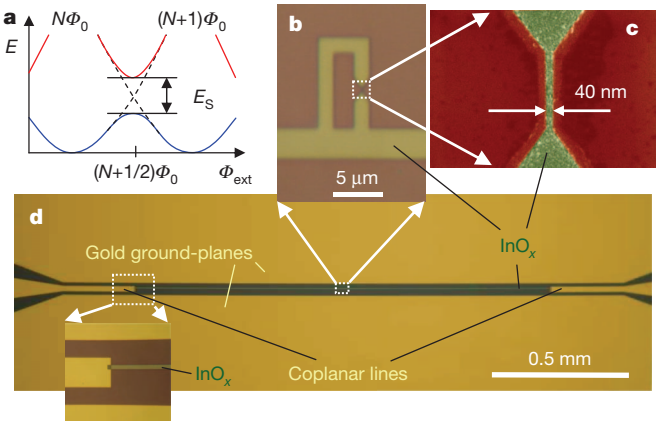

Figure 1 | The device. **a**, Energies of the loop versus external flux, Φ_{ext}. Blue and red lines: ground and excited energy levels, respectively. The degeneracy between states with N and $N+1$ flux quanta (Φ_0), seen at $\Phi_{ext} = (N+1/2)\Phi_0$, is lifted by the phase-slip energy, E_S. **b**, InO_x loop with a narrow wire segment on the right side is attached to the resonator (horizontal line) at the bottom. **c**, False-colour scanning-electron micrograph of the narrow InO_x segment. **d**, Step-impedance resonator, comprising a 3-μm-wide InO_x strip with wave impedance $Z_1 \approx 1{,}600\,\Omega$ galvanically coupled to a gold coplanar line with impedance $Z_0 = 50\,\Omega$. The boundaries of the resonator are defined by the strong impedance mismatch ($Z_1 \gg Z_0$).

[1]NEC Green Innovation Research Laboratories, 34 Miyukigaoka, Tsukuba, Ibaraki, 305-8501, Japan. [2]The Institute of Physical and Chemical Research (RIKEN), 34 Miyukigaoka, Tsukuba, Ibaraki, 305-8501, Japan. [3]Center for Materials Theory, Department of Physics and Astronomy, Rutgers University, 136 Frelinghuysen Road, Piscataway, New Jersey 08854, USA. [4]Department of Physics, Lancaster University, Lancaster LA1 4YB, UK. [5]University of Jyväskylä, Department of Physics, PB 35, 40014 Jyväskylä, Finland. [6]Moscow State University, Institute of Nuclear Physics, Leninskie gory, GSP-1, Moscow 119899, Russia. [7]Department of Condensed Matter Physics, Weizmann Institute of Science, Rehovot 76100, Israel.

enhanced in narrow wires with a small number of effective conductive channels, $N_{ch} = R_K/R_\xi$, where R_ξ is the resistance of a wire of length ξ and $R_K = (h/e^2)$. The phase-slip amplitude decreases with N_{ch} as $E_S \propto \exp(-aN_{ch})$ (refs 20, 21), where a is a numerical parameter of order 1. Our data are consistent with $a \approx 0.3$ for $R_\xi = 1\,k\Omega$ and $\xi = 10\,nm$ (Supplementary Information). Thus, E_S is expected to be sizeable in strongly disordered, quasi-one-dimensional superconducting wires. But a high degree of disorder may also enhance Coulomb repulsion between electrons, and turn the superconductor into a dissipative normal metal[22]. The ideal materials for observation of CQPS should therefore form localized, pre-formed pairs even before they become superconducting[23–25]. Such behaviour has been observed in amorphous InO_x and TiN thin films[26,27].

Our loops (Fig. 1b) are fabricated from a 35-nm-thick superconducting InO_x film with $\xi = 10$–$30\,nm$ (ref. 28), using electron-beam lithography. The uncertainty in the magnitude of ξ is due to the poor applicability of BCS theory (see Supplementary Information). Each loop contains a narrow wire segment, about 40 nm wide and 400 nm long (Fig. 1c). This wire is reasonably homogeneous, varying in width by less than 10 nm. We have characterized identical wires and films, fabricated by the same process, using d.c. transport measurements. The film exhibits a superconducting transition at $T_c = 2.7\,K$. The sheet resistance R_{sq} of the wide films, measured slightly above T_c, is 1.7 kΩ, which gives a rough (BCS) estimate of the sheet inductance as $L_{sq} \approx \hbar R_{sq}/\pi\Delta \approx 0.7\,nH$ (ref. 13) (for $\Delta \approx 0.5\,meV$; ref. 26) for the wide sections of the loops.

To measure the loops, we incorporate them in a step-impedance coplanar resonator: a strip line of InO_x of length $L = 1.5\,mm$ and width $W = 3\,\mu m$, galvanically connected to two gold coplanar lines (with impedance $Z_0 = 50\,\Omega$) at the ends (Fig. 1d). We estimate the effective wave impedance of the line to be $Z_1 = \sqrt{l_1/c_1} \approx 1.6\,k\Omega$, with specific inductance $l_1 = L_{sq}/W \approx 2.3 \times 10^{-4}\,H\,m^{-1}$ and specific capacitance $c_1 \approx 0.85 \times 10^{-10}\,F\,m^{-1}$). Because $Z_1 \gg Z_0$, the strong mismatch results in standing wave formation with maximal current at the boundaries: $I(x) = I_m \cos(\pi m x/L)$, where x is the coordinate along the resonator ($0 \le x \le L$). The resonance frequency of the mth mode f_m ($m = 1,2,3...$) is given by $f_m \approx mv/2L = m \times 2.4\,GHz$, where $v = (l_1 c_1)^{-1/2} \approx 7.2 \times 10^6\,m\,s^{-1}$ is the group velocity in the resonator. The energy decay rate in such a resonator is $\kappa \approx (4Z_0/Z_1)(v/L)$, which limits the power peak width to $\kappa/2\pi \approx 0.1\,GHz$.

Our main results are as follows. Figure 2a shows the power transmission coefficient $|t|^2$ through the resonator at a temperature of 40 mK. The peaks correspond to $m = 3,4,5$, with resonance frequencies $f_3 = 6.65\,GHz$, $f_4 = 9.08\,GHz$ and $f_5 = 11.00\,GHz$ (close to our estimates above). The actual peak widths (full-width at half-maximum) are approximately 250 MHz ($= \kappa/2\pi$), which is twice as large as that expected from the loading loss. This is probably due to an extra loss in the gold ground-plane films. Our loops located in the middle of the resonator ($x = L/2$) are coupled only to the odd modes m, for which the current defined by $I_{mw} = I_m \cos(\pi m/2)$ is non-zero.

To detect the superposition of flux states we measure transmission t through the resonator at f_m versus B_{ext}. The transmission does not depend on B_{ext} at the third and fifth peaks. However, at the fourth mode peak, t exhibits well pronounced periodic structure: sharp negative dips in the amplitude $|t|$, and in the phase rotation $\arg(t)$, as shown in Fig. 2b. The period, $\Delta B = 0.061\,mT$, corresponds with high accuracy to one flux quantum, Φ_0, through the area $S = 32\,\mu m^2$ of the loop shown in Fig. 1b, with a 40-nm-wide wire. Note that there is a small (~5%) uncertainty in the loop area, owing to the finite width of the lines. Each resonator contains five loops, with nanowire widths 40, 60, 80, 100 and 120 nm. The loops differ slightly in area, varying by 10–12% from one to another. No CQPS-related signals are found from the samples with nanowire segments wider than 40 nm, indicating that in these loops $E_S/h < 1\,GHz$, in good agreement with our prediction that E_S will be suppressed by more than a factor of 10 with an increase of 20 nm in the nanowire width. (See Supplementary Information.)

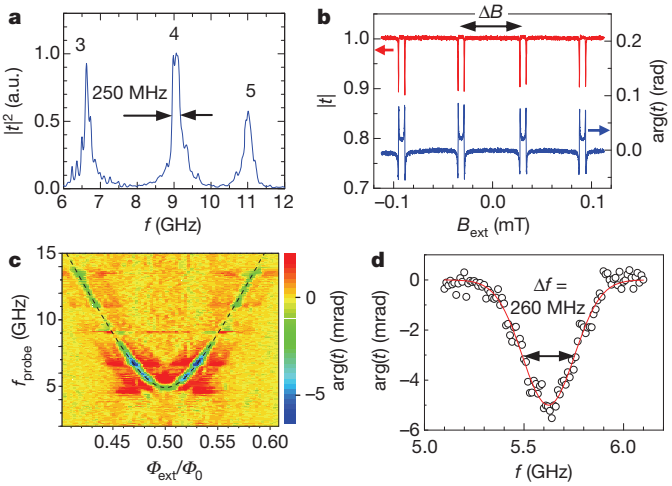

Figure 2 | Experimental data. **a**, Power transmission through the resonator, measured within the bandwidth of our experimental setup. Peaks in transmission power coefficient, $|t|^2$, correspond to resonator modes, with mode number m indicated for each peak. a.u., arbitrary units. **b**, Transmission through the resonator as function of external magnetic field B_{ext} at $m = 4$ ($f_4 = 9.08\,GHz$). The periodic structure in amplitude ($|t|$) and phase ($\arg(t)$) corresponds to the points where the lowest-level energy gap $\Delta E/h$ matches f_4. The period $\Delta B = 0.061\,mT$ ($= \Phi_0/S$) indicates that the response comes from the loop (shown in Fig. 1**b**), with the effective loop area $S = 32\,\mu m^2$. **c**, The two-level spectroscopy line obtained in two-tone measurements. The phase of transmission, $\arg(t)$, through the resonator at f_4 is monitored, while another tone with frequency f_{probe} from an additional microwave generator, and B_{ext}, are independently swept. The plot is filtered to eliminate the contribution of other resonances ($2 \le m \le 6$), visible as horizontal red features. The dashed line is the fit to the energy splitting, with $\Delta E/h = 4.9\,GHz$, $I_p = 24\,nA$. **d**, The resonant dip is measured at $\Phi/\Phi_0 = 0.52$. The red curve is the Gaussian fit.

Although the coupling of our loop to the resonator ($g/h \approx 10\,MHz$) is weak ($g << \hbar\kappa$), we were able to perform spectroscopy measurements by monitoring resonator transmission[29,30] while scanning B_{ext} and the frequency, f_{probe}, of an additional probe microwave tone. The transmission phase plot shows the resonance excitation of the two-level system (Fig. 2c). The obtained structure is distorted by periodic resonances at f_m (seen as red horizontal features), and the resulting picture is plotted after filtering out these resonances. The green–blue line corresponds to the expected energy splitting, which is well fit by $\Delta E = \sqrt{(2I_p\delta\Phi)^2 + E_S^2}$ (dashed line), with the fitting parameters $E_S/h < 4.9\,GHz$ and $I_p = 24\,nA$, corresponding to $L_k = 42\,nH$.

The exact splitting at the degeneracy point $\delta\Phi = 0$ happens to nearly coincide with $f_2 \approx 4.8\,GHz$, distorting the line shape. Figure 2d shows the resonant peak at $\Phi_{ext} = 0.52\,\Phi_0$, slightly away from the degeneracy point, where the resonant frequency $\Delta E/h \approx 5.6\,GHz$ is between f_1 and f_2. The spectroscopy peak is well fit by a Gaussian, $A\exp\left[-\frac{1}{2}\left(\frac{f-\Delta E/h}{\Delta f}\right)^2\right]$, with $\Delta f = 260\,MHz$. This demonstrates coherent coupling between the flux states in the loop. An interesting question, which requires further study, is the mechanism of decoherence in this type of system. At this stage, we can only conjecture that the shape suggests peak broadening due to low-frequency Gaussian noise, rather than relaxation.

We now discuss the relation between the measured and expected properties of the system. The total loop resistance R (at $T > T_c$) is the sum of the resistances of the wide section (estimated from R_{sq}) and of the nanowire, $R_w \approx 30\,k\Omega$, deduced from the d.c. measurements of identical samples. We estimate $R \approx 55\,k\Omega$. As one might expect, the effective sheet resistance of the narrow wires is higher than R_{sq}—in our case, by a factor of 1.8. The BCS estimate of the inductance of the whole loop gives $L_k \approx 23\,nH$. Close to the superconductor–insulator transition

(SIT), R rises continuously with decreasing temperature before the onset of superconductivity, whereas L_k diverges at the transition. Arguing by continuity, BCS theory should underestimate L_k in the strongly disordered superconductors (see Supplementary Information). We underestimate L_k in our films by a factor of 1.8, which is very reasonable for the superconductors close to the SIT.

Another measure of the wire quality is the value of its critical current. For a BCS superconductor, the maximal supercurrent[13] is $I_c \approx 0.75\Delta/eR_\xi$ (Supplementary Information). Taking into account that in the vicinity of the SIT, I_c is overestimated by at least the same factor of 1.8 (as with L_k), we find $I_c \leq 280$–90 nA, for $\xi = 10$–30 nm. The measured value, $I_c = 100$ nA, is in full agreement with these expectations.

The quantitative estimate of the QPS amplitude is less accurate than for kinetic inductance or critical current, owing to its exponential dependence on sample and material parameters. Moreover, in the BCS approximation, QPS amplitude explicitly depends on ξ, which is not well defined close to the SIT. Rough estimates based on ref. 15 give values of ~5–20 GHz for $\xi = 10$ nm; our calculations, based on the measured value of the sheet kinetic inductance, yield $E_S \approx 10$ GHz, in agreement with the data (see Supplementary Information).

We have obtained additional evidence for CQPS, as follows. In addition to the data presented here for a single sample, we observed very similar results in two other samples fabricated from the same InO_x film. One of those samples was measured in the step-impedance resonator described above, and the other in an open-line configuration[19]. In all three samples, we found resonances with close values of persistent current, and level splitting E_S/h equal to 4.9, 5.8 and 9.5 GHz, respectively. The variation in E_S is surprisingly low (given its exponential dependence on parameters), and is in agreement with expectations (see Supplementary Information). This reproducibility is a strong argument against an alternative interpretation of the results based on unintentional formation of a rogue Josephson junction somewhere in the wire. Second, as in a charge qubit (which is dual to our system with CQPS), the energy difference between the two lowest states in the loop asymptotically approaches linear dependence, $\Delta E = 2I_p\delta\Phi$, at $\Delta E \gg E_S$. In our experiments, we are able to trace the two-level system resonance up to $|\delta\Phi| \geq 0.5\Phi_0$ and $\Delta E \approx 77$ GHz (Fig. 3). This linear dependence, without any observable splitting at $\Phi = 0$ and Φ_0 (corresponding to the second-order 4π-process), indicates a linear inductance in our system, rather than a nonlinear one originating in a rogue Josephson junction. To support this statement, we present simulations of the spectroscopy lines (dotted cyan lines in Fig. 3) for a radio-frequency-SQUID qubit with a single Josephson junction (with $I_c = 100$ nA), and with capacitance and linear inductance adjusted to provide the best fit of our spectroscopy data. The simulations show a significant rounding at $\Phi = 0$ and Φ_0, owing to the nonlinear Josephson inductance, in qualitative disagreement with our results. These arguments allow us to exclude a rogue Josephson junction formed in our device; however, we cannot distinguish a number of interfering phase slip locations in the wire, if, for example, the wire is not uniform.

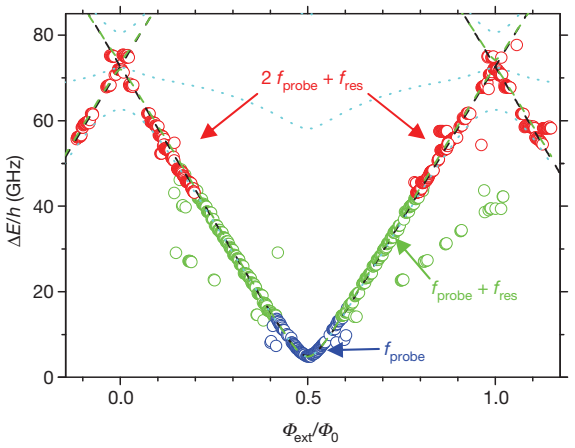

Figure 3 | Spectroscopy of the system across a wide range of flux and frequency. The spectroscopy response is obtained by measuring the transmission amplitude and phase through the resonator at $f_4 = 9.08$ GHz, while the frequency of the additional microwave tone f_{probe} is swept. Depending on the range, the two-level system excitation frequency $\Delta E/h$ is derived from the direct (single-photon) excitation $\Delta E/h = f_{probe}$ (blue circles), the two-photon process $\Delta E/h = f_{probe} + f_4$ (green circles), or the three-photon process $\Delta E/h = 2f_{probe} + f_4$ (red circles). With these methods, using $f_{probe} \leq 35$ GHz, we could trace $\Delta E/h$ up to about 77 GHz. The dashed black line is the calculated energy splitting, $\Delta E/h = \frac{\sqrt{(2I_p\delta\Phi)^2 + E_S^2}}{h}$, with $E_S = 4.9$ GHz and $I_p = 24$ nA. Perfect agreement of the experimental data with the calculated energy bands supports our interpretation; the quantum states of the system correspond to the superposition of the two adjacent flux states induced by CQPS. The rare scattered points result from noise, resonator resonances and higher-order excitation processes. For comparison, the additional dotted cyan lines show the expected behaviour of a radio-frequency-SQUID qubit with $E_J/h = 50$ GHz ($I_c = 100$ nA), capacitance $C = 1.1$ fF and inductance $L = 38$ nH, which qualitatively disagrees with our data at the degeneracy points $\Phi_{ext} = 0$ and $\Phi_{ext} = \Phi_0$.

Received 24 October 2011; accepted 3 February 2012.

1. Mooij, J. E. & Nazarov, Yu. V. Superconducting nanowires as quantum phase-slip junctions. *Nature Phys.* **2,** 169–172 (2006).
2. Tinkham, M. *Introduction to Superconductivity* (McGraw-Hill, 1996).
3. Averin, D. V., Zorin, A. B. & Likharev, K. K. Bloch oscillations in small Josephson junction. *Zh. Eksp. Teor. Fiz.* **88,** 407–412 (1984).
4. Giordano, N. Evidence for macroscopic quantum tunnelling in one-dimensional superconductors. *Phys. Rev. Lett.* **61,** 2137–2140 (1988).
5. Bezryadin, A., Lau, C. N. & Tinkham, M. Quantum suppression of superconductivity in ultrathin nanowires. *Nature* **404,** 971–974 (2000).
6. Zgirski, M., Riikonen, K.-P., Touboltsev, V. & Arutyunov, K. Yu. Quantum fluctuations in ultranarrow superconducting aluminum nanowires. *Phys. Rev. B* **77,** 054508 (2008).
7. Lehtinen, J. S., Sajavaara, T., Arutyunov, K., Yu. & Vasiliev, A. Evidence of quantum phase slip effect in titanium nanowires. Preprint at ⟨http://arxiv.org/abs/1106.3852⟩ (2011).
8. Hongisto, T. T. & Zorin, A. B. Single charge transistor based on superconducting nanowire in high impedance environment. *Phys. Rev. Lett.* **108,** 097001 (2012).
9. Matveev, K. A., Larkin, A. I. & Glazman, L. I. Persistent current in superconducting nanorings. *Phys. Rev. Lett.* **89,** 096802 (2002).
10. Hriscu, A. M. & Nazarov, Yu. V. Model of a proposed superconducting phase slip oscillator: A method for obtaining few-photon nonlinearities. *Phys. Rev. Lett.* **106,** 077004 (2011).
11. Hriscu, A. M. & Nazarov, Yu. V. Coulomb blockade due to quantum phase-slips illustrated with devices. *Phys. Rev. B* **83,** 174511 (2011).
12. Vanevic, M. & Nazarov, Yu. V. Quantum phase slips in superconducting wires with weak links. Preprint at ⟨http://arxiv.org/abs/1108.3553⟩ (2011).
13. Mooij, J. E. & Harmans, C. J. P. M. Phase-slip flux qubits. *N. J. Phys.* **7,** 219 (2005).
14. Little, W. A. Decay of persistent current in small superconductors. *Phys. Rev.* **156,** 396–403 (1967).
15. Arutyunov, K. Yu, Golubev, D. S. & Zaikin, A. D. Superconductivity in one dimension. *Phys. Rep.* **464,** 1–70 (2008).
16. Manucharyan, V. E. *et al., Phys. Rev. B* **85,** 024521 (2012).
17. Pop, I. M. *et al.* Experimental demonstration of Aharonov-Casher interference in a Josephson junction circuit. Preprint at ⟨http://arxiv.org/abs/1104.3999⟩ (2011).
18. Arutyunov, K. Yu, Hongisto, T. T., Lehtinen, J. S., Leino, L. I. & Vasiliev, A. L. Quantum phase-slip phenomenon in ultra-narrow superconducting nanorings. *Sci. Rep.* **2,** 293 (2012).
19. Astafiev, O. *et al.* Resonance fluorescence of a single artificial atom. *Science* **327,** 840–843 (2010).
20. Zaikin, A. D., Golubev, D. S., van Otterlo, A. & Zimanyi, G. T. Quantum phase slips and transport in ultrathin superconducting wires. *Phys. Rev. Lett.* **78,** 1552–1555 (1997).
21. Golubev, D. S. & Zaikin, A. D. Quantum tunneling of the order parameter in superconducting nanowires. *Phys. Rev. B* 014504 (2001).
22. Finkel'stein, A. M. Suppression of superconductivity in homogeneously disordered systems. *Physica B* **197,** 636–648 (1994).
23. Feigel'man, M. V., Ioffe, L. B., Kravtsov, V. E. & Cuevas, E. Fractal superconductivity near localization threshold. *Ann. Phys.* **325,** 1390–1478 (2010).
24. Feigel'man, M. V., Ioffe, L. B., Kravtsov, V. E. & Yuzbashyan, E. A. Eigenfunction fractality and pseudogap state near the superconductor-insulator transition. *Phys. Rev. Lett.* **98,** 027001 (2007).
25. Feigel'man, M. V., Ioffe, L. B. & Mezard, M. Superconductor-insulator transition and energy localization. *Phys. Rev. B* **82,** 184534 (2010).

26. Sacépé, B. *et al.* Localization of preformed Cooper pairs in disordered superconductors. *Nature Phys.* **7,** 239–244 (2011).
27. Sacépé, B. *et al.* Pseudogap in a thin film of a conventional superconductor. *Nature Commun.* **1,** 140 (2010).
28. Johansson, A., Sambandamurthy, G., Shahar, D., Jacobson, N. & Tenne, R. Nanowire acting as superconducting quantum device. *Phys. Rev. Lett.* **95,** 116805 (2005).
29. Wallraff, A. *et al.* Approaching unit visibility for control of a superconducting qubit with dispersive readout. *Phys. Rev. Lett.* **95,** 060501 (2005).
30. Abdumalikov, A. A. Jr, Astafiev, O. V., Nakamura, Y., Pashkin, Yu. A. & Tsai, J. S. Vacuum Rabi splitting due to strong coupling of a flux qubit and a coplanar-waveguide resonator. *Phys. Rev. B* **78,** 180502 (2008).

Supplementary Information is linked to the online version of the paper at www.nature.com/nature.

Acknowledgements We are grateful to M. Feigel'man, J. Mooij and Y. Nazarov for discussions. This work was supported by Funding Program for World-Leading Innovative R&D on Science and Technology (FIRST), MEXT KAKENHI "Quantum Cybernetics", Ministry of Science and Education of Russian Federation grant 2010-1.5-508-005-037. L.B.I. was supported by ARO W911NF-09-1-0395, DARPA HR0011-09-1- 0009 and NIRT ECS-0608842. D.S. and O.C. were supported by Minerva Fund.

Author Contributions O.V.A. planned the experiment, designed and fabricated the samples, performed measurements and data analysis. L.B.I. came up with the idea of using materials close to the SIT and provided theoretical support. S.K. fabricated the sample and contributed to understanding the data . Yu.A.P. participated in discussions of the experiment. K.Yu.A. triggered the research direction and suggested the realization of the phase-slip qubit. D.S. and O.C. fabricated the InO_x films. J.S.T. discussed the data and provided support for the work within the FIRST and KAKENHI projects. O.V.A. wrote the manuscript with feedback from all authors, including significant contributions from L.B.I. and K.Yu.A.

Author Information Reprints and permissions information is available at www.nature.com/reprints. The authors declare no competing financial interests. Readers are welcome to comment on the online version of this article at www.nature.com/nature. Correspondence and requests for materials should be addressed to O.V.A. (astf@zb.jp.nec.com).